In-Plane Saturable Absorption of Graphene on a Silicon Slot Waveguide

Jiaqi Wang[1], Zhenzhou Cheng[2], Hon Ki Tsang[1], and Chester Shu[1]
[1]Department of Electronic Engineering, The Chinese University of Hong Kong, Shatin, N.T., Hong Kong
[2]Department of Chemistry, University of Tokyo, Hongo 7-3-1, Bunkyo-ku, Tokyo, Japan
jqwang@ee.cuhk.edu.hk

Abstract: *We studied the saturable absorption in 17-micrometer long graphene-on-silicon slot waveguide at 1550nm wavelength. Saturation behavior was observed beginning from 20 pJ input optical pulse energy. The transmission increased by 44% at 167 pJ input.*
Keywords: *(Silicon photonics, slot waveguide, graphene, nonlinear optics, integrated optics)*

I. Introduction

With the features of ultrahigh electron mobility, zero bandgap and tunable absorption [1], [2], graphene is promising for many photonic and optoelectronic applications, such as electro-absorption modulators [3], high-speed and broadband photodetectors [4-6], and mode-locked fiber lasers extending to the mid-infrared spectral region [7]. Graphene has been suggested as a material with giant $\chi^{(3)}$ nonlinearities. Strong third-order nonlinear response has been demonstrated in the graphene-on-silicon photonic crystal cavity [8]. Besides, the ultrafast carrier dynamics along with the linear electron/hole dispersion make graphene an ideal solution for ultrafast and broadband saturable absorbers. The band filling effect causes the absorption of graphene to decrease at high power levels. With chemical vapor deposition (CVD) grown graphene [9] or graphene-polymer composite [10] acting as a saturable absorber and adhered to the fiber end, ultrafast pulsed fiber lasers have been demonstrated.

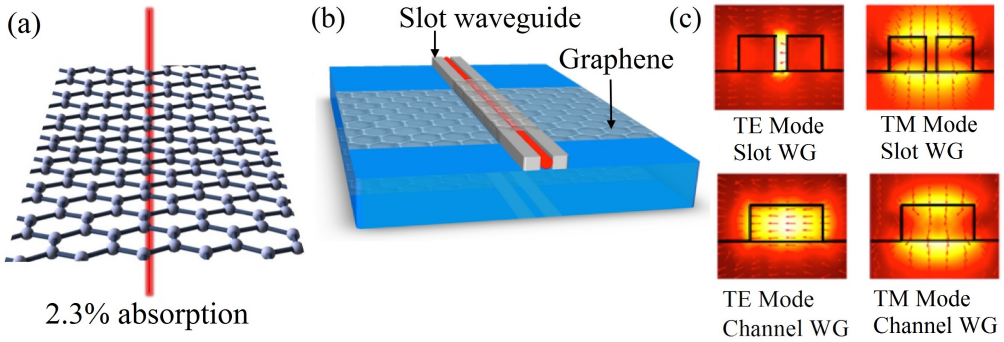

Fig. 1 (a) Graphene absorption for the normal incidence case. (b) Schematic illustration of the graphene-on-silicon slot waveguide. (c) Electrical field distribution of the TE/TM slot waveguides and channel waveguides with graphene integrated on top.

With the two-dimensional nature, graphene is suitable to be integrated on the photonic integrated circuits (PICs) [11]. The interaction of the evanescent field with graphene along the waveguide can dramatically increase the optical absorption towards ~100%, comparing to 2.3% absorption for the normal incidence case, as shown in Fig. 1 (a) and (b). In-plane nonlinear absorption of graphene-on-silicon channel waveguide structures has been previously studied [12-14]. Here we report the characterization of saturable absorption on silicon slot waveguides for possible application in mode-locked lasers on-chip [15-17] by using slot-waveguide integrated graphene saturable absorbers. Compared to conventional channel waveguides, the slot waveguide is able to guide and confine higher intensity of light in the nano-meter size low index slot due to the discontinuity of electrical field at the high-index contrast interface. The electrical field distributions of the fundamental silicon TE/TM slot waveguides and channel waveguides with graphene integrated on top are shown in Fig. 1 (c). The in-plane graphene-light interaction is stronger for the TE mode in graphene-on-slot waveguides, comparing to that in graphene-on-channel waveguides [18]. The graphene-on-silicon slot waveguide can further reduce the device footprint and eliminate the need on the growth of large-area high quality graphene. Moreover, the graphene-on-silicon slot waveguide is suitable for nonlinear applications, since there is no silicon present at the location of peak optical intensity, thus avoiding two-photon absorption (TPA) and TPA induced free carrier absorption loss from the silicon waveguide [19], [20].

We transferred CVD grown monolayer graphene onto the silicon vertical slot waveguide devices and tailored the length of graphene on top of the waveguide. The 17-μm long graphene integrated on top gives rise to ~15.6 dB absorption loss in the silicon slot waveguide. The nonlinear absorption behavior was studied by using a gain-switched short pulse laser at 1.55 μm wavelength. The transmission increased rapidly when the coupled pulse energy was larger than 20 pJ. When the pulse energy was above 167 pJ, the transmission was 44% larger than that at the low power regime.

II. FABRICATION AND EXPERIMENTAL RESULTS

The TE mode silicon slot waveguide consists of two silicon ridge waveguides separated by a 70-nm wide air slot. According to our previous study [18], the fundamental TE mode slot waveguide has the largest optical absorption loss among the TE/TM mode channel waveguides and TE/TM slot waveguides. A Y junction is used as the mode converter between the channel waveguide and the slot waveguide. The focusing subwavelength gratings [21], [22] are applied to couple the TE mode in and out of the waveguide. The silicon devices were fabricated on a commercial silicon-on-insulator (SOI) wafer which contains 250-nm silicon on a 3-μm buried oxide. The slot waveguides and subwavelength gratings were defined by electronic beam lithography (EBL) followed by deep reactive-ion etching. The commercial CVD grown graphene was wet transferred onto the silicon devices. The graphene on top of the waveguide was tailored to 17 μm by using EBL and O_2 plasma etching. The fabricated grating coupler and graphene-on-silicon slot waveguide are shown in the scanning electronic microscopy (SEM) images in Fig.2 (a) and (b), respectively. Through the contrast in Fig. 2 (b), the area with and without graphene can be clearly identified. Raman spectroscopy was used to verify the monolayer graphene. The Raman spectrum of the graphene integrated on the slot waveguide is measured using a 512 nm laser and the result is shown in Fig. 2 (c). The ratio of G peak (1588 cm^{-1}) to 2D peak (2690 cm^{-1}) is smaller than 0.5, indicating the monolayer graphene structure [23], [24]. The graphene introduces ~15.6 dB absorption loss in the low power measurement (-10 dBm input power).

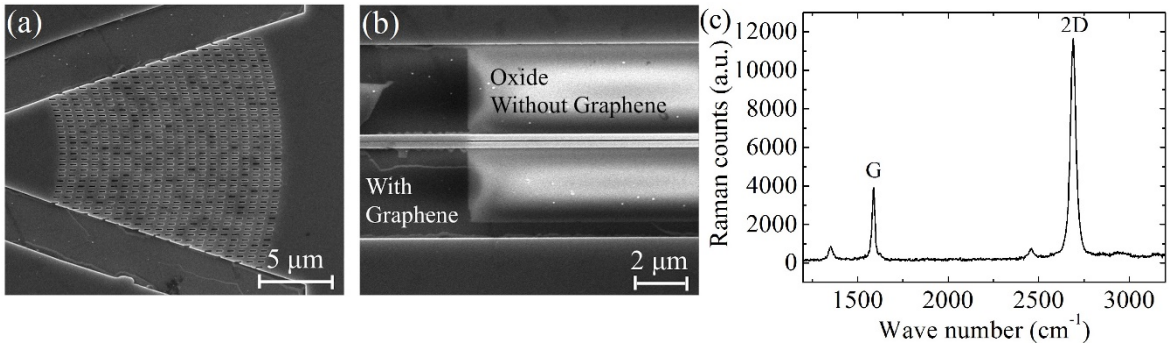

Fig. 2 (a) SEM image of the fabricated subwavelength grating coupler. (b) SEM image of the graphene-on-silicon slot waveguide. The area with and without graphene can be clearly identified through the contrast of the image. (c) Raman spectrum of the graphene integrated on top of the silicon slot waveguide.

The setup of the saturable absorption measurement is shown in Fig. 3 (a). The laser source was a gain-switched semiconductor laser with ~50 ps pulse width and 1 MHz repetition rate centered at 1555.65 nm. The laser was amplified and the output was subsequently filtered by an optical bandpass filter. A 5% tap was used to monitor the input power. The other 95% was coupled into the graphene-on-silicon slot waveguide through a TE mode subwavelength grating with a coupling efficiency of 30%. The transmission of the graphene-on-silicon slot waveguide as a function of pulse energy is shown in Fig. 3 (b). At low input pulse energy, the transmission is independent of the input energy. At high input level, the increased concentration of excited electrons results in band filling and begins to block some absorption. The transmission starts to increase rapidly at coupled pulse energy above 20 pJ (376mW peak power). When the coupled pulse energy is increased to 167 pJ (3.14 W peak power), the transmission was 44% larger than that in the low power regime.

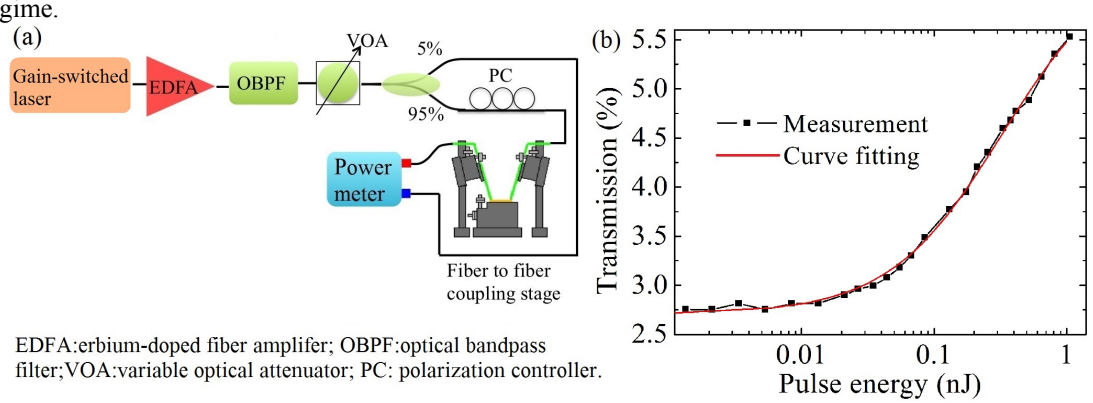

Fig. 3 (a) Schematic illustration of the saturable absorption measurement. (b) Transmission of the graphene-on-silicon slot waveguide at different input optical pulse energy.

The transmission of the graphene-on-silicon slot waveguide is described by $T=e^{-\alpha L}$, where α is the absorption coefficient and L=17 μm is the length of the graphene. The two-stage saturable absorption model is widely used to describe the nonlinear absorption in two-dimensional quantum wells. It can be adopted to approximate the nonlinear absorption in graphene [9]. The absorption coefficient $\alpha(E)$, where E is optical pulse energy, is described by

$$\alpha(E) = \frac{\alpha_S}{(1+\frac{E}{E_S})} + \alpha_{NS} \qquad (1)$$

where α_S and α_{NS} are the saturable and non-saturable absorption components, E_S is the saturation pulse energy. The non-saturable absorption component is mainly caused by scattering loss in the silicon slot waveguide. The fitting curve is shown in Fig. 3 (b), and α_S, α_{NS} and E_S are obtained as 0.05 μm^{-1}, 0.019 μm^{-1}, and 213 pJ, respectively. The saturation energy is relatively low, comparing to the 3.9 nJ in the case of graphene-on-silicon channel waveguide [14]. The reason is that the optical interaction is significantly enhanced in the graphene-on-slot waveguide configuration and a smaller area of graphene is present on the slot waveguide.

III. CONCLUSION

A graphene-on-silicon slot waveguide structure is proposed and demonstrated to enhance the optical interaction between graphene and the evanescent field of the waveguide. The nonlinear absorption of the graphene-on-silicon slot waveguide is studied with a gain-switched short pulse laser. Saturable absorption is observed at relatively low input pulse energy of 20 pJ. The observation is explained by the enhanced optical interaction as well as the small area of graphene over the slot waveguide. The graphene-on-silicon slot waveguide can have potential applications in realizing ultrafast on-chip mode-locked lasers and nonlinear optical processing.

ACKNOWLEDGMENT

This work was supported by Hong Kong Research RGC GRF grants CUHK 416213 and 14206614.

REFERENCES

[1] M. Freitag, et al. "Photoconductivity of biased graphene." Nat. Photon., 7, 53 (2013).
[2] D. Kim, et al, "Work function engineering of graphene anode by bis (trifluoromethanesulfonyl) amide doping for efficient polymer light emitting diodes," Adv. Funct. Mater, 23, 5049-5055 (2013).
[3] M. Liu, et al, "A graphene-based broadband optical modulator," Nature, 474, 64-67 (2011).
[4] X. Gan, et al, "Chip-integrated ultrafast graphene photodetector with high responsivity," Nat. Photon., 7, 883-887 (2013).
[5] A. Pospischil, et al, "CMOS-compatible graphene photodetector covering all optical communication bands," Nat. Photon., 7, 892-896 (2013).
[6] X. Wang, et al, "High responsivity graphene/silicon heterostructure waveguide photodetectors", Nat. Photon.,7, 888-891 (2013).
[7] G. Zhu, et al, "Graphene Mode-Locked Fiber Laser at 2.8 μm," IEEE Phot. Tech. Lett.,28, 7-10 (2016).
[8] T. Gu, et al, "Regenerative oscillation and four-wave mixing in graphene optoelectronics," Nat. Photon., 6, 554-559 (2012).
[9] Q. Bao, et al, "Atomic layer graphene as a saturable absorber for ultrafast pulsed lasers," Adv. Funct. Mater, 19, 3077-3083 (2009).
[10] Z. Sun, et al, "Graphene mode-locked ultrafast laser," ACS Nano 4, 803-810 (2010).
[11] R. Kou, et al, "Influence of graphene on quality factor variation in a silicon ring resonator," Appl. Phys. Lett., 104, 091122 (2014).
[12] K. Alexander, et al, "Electrically controllable saturable absorption in hybrid graphene-silicon waveguides," In CLEO: Science and Innovations, STh4H-7, Optical Society of America (2015).
[13] Z. Cheng, et al, "In-plane optical absorption and free carrier absorption in graphene-on-silicon waveguides," IEEE J. Sel. Top. Quantum Electron., 20, 43-48 (2014).
[14] Z. Shi, et al, "In-plane saturable absorption of graphene on silicon waveguides," In Conference on Lasers and Electro-Optics/Pacific Rim, WA4_3, Optical Society of America (2013).
[15] Y. Urino, et al, "Demonstration of 12.5-Gbps optical interconnects integrated with lasers, optical splitters, optical modulators and photodetectors on a single silicon substrate," Opt. Express, 20, B256-B263 (2012).
[16] Y.D.Yang, et al, "Direct-modulated waveguide-coupled microspiral disk lasers with spatially selective injection for on-chip optical interconnects," Opt. Express, 22, 824-838 (2014).
[17] K. Ogawa, "High-speed silicon-based integrated optical modulators for optical-fiber telecommunications," In SPIE OPTO, 899010-899010, International Society for Optics and Photonics (2014).
[18] Z. Cheng, et al, "Graphene absorption enhancement using silicon slot waveguides," In Photonics Conference, 186-187, IEEE (2015).
[19] D. Marpaung, et al, "Nonlinear integrated microwave photonics," J. Lightwave Technol., 32, 3421-342720 (2014).
[20] M. Foster, et al, "Broad-band optical parametric gain on a silicon photonic chip," Nature, 441,960-963 (2006).
[21] L. Vivien, et al, "Light injection in SOI microwaveguides using high-efficiency grating couplers," J. Lightwave Technol., 10, 3810-381524 (2006).
[22] Z. Cheng, et al, "Focusing subwavelength grating coupler for mid-infrared suspended membrane waveguide," Opt. Lett., 37, 1217-1219 (2012).
[23] L. Xiao, et al, "Low-temperature Raman G-mode of plasmonic-graphene hybrid platform," In CLEO: Science and Innovations, JTu4A-9, Optical Society of America (2014).
[24] A. C. Ferrari, et al, "Raman spectrum of graphene and graphene layers," Phys. Rev. Lett., 97, 187401 (2006).